Graphene oxide disruption of homeostasis and regeneration processes in freshwater planarian Dugesia japonica via intracellular redox deviation and apoptosis

Xie, Changjian; Li, Xiaowei; Guo, Zhiling; Dong, Yuling; Zhang, Shujing; Li, Ao; Ma, Shan; Xu, Jianing; Pang, Qiuxiang; Peijnenburg, Willie J.G.M.; Lynch, Iseult; Zhang, Peng

DOI:
10.1016/j.ecoenv.2022.114431

Document Version
Publisher's PDF, also known as Version of record

Citation for published version (Harvard):
Xie, C, Li, X, Guo, Z, Dong, Y, Zhang, S, Li, A, Ma, S, Xu, J, Pang, Q, Peijnenburg, WJGM, Lynch, I & Zhang, P 2023, 'Graphene oxide disruption of homeostasis and regeneration processes in freshwater planarian *Dugesia japonica* via intracellular redox deviation and apoptosis', *Ecotoxicology and Environmental Safety*, vol. 249, 114431. https://doi.org/10.1016/j.ecoenv.2022.114431

Ecotoxicology and Environmental Safety 249 (2023) 114431

Contents lists available at ScienceDirect

Ecotoxicology and Environmental Safety

journal homepage: www.elsevier.com/locate/ecoenv

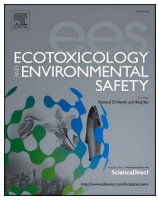

Graphene oxide disruption of homeostasis and regeneration processes in freshwater planarian *Dugesia japonica* via intracellular redox deviation and apoptosis

Changjian Xie [a], Xiaowei Li [a], Zhiling Guo [b], Yuling Dong [a], Shujing Zhang [a], Ao Li [a], Shan Ma [d], Jianing Xu [a], Qiuxiang Pang [a,*], Willie J.G.M. Peijnenburg [e,f], Iseult Lynch [b], Peng Zhang [b,c,**]

[a] School of life Sciences and medicine, Shandong University of Technology, Zibo 255000, Shandong, China
[b] School of Geography, Earth and Environmental Sciences, University of Birmingham, Edgbaston, Birmingham B15 2TT, United Kingdom
[c] Department of Environmental Science and Engineering, University of Science and Technology of China, Hefei 230026, China
[d] Zibo Environment Monitoring Center, Zibo 25500, Shandong, China
[e] Institute of Environmental Sciences (CML), Leiden University, Einsteinweg 2, 2333 CC Leiden, the Netherlands
[f] National Institute of Public Health and the Environment (RIVM), Center for Safety of Substances and Products, Bilthoven, the Netherlands

ARTICLE INFO

Edited by: Professor Bing Yan

Keywords:
Graphene oxide
Planarian
Development toxicity
Stem cell
Regeneration
Oxidative stress

ABSTRACT

The aquatic system is a major sink for engineered nanomaterials released into the environment. Here, we assessed the toxicity of graphene oxide (GO) using the freshwater planarian *Dugesia japonica*, an invertebrate model that has been widely used for studying the effects of toxins on tissue regeneration and neuronal development. GO not only impaired the growth of normal (homeostatic) worms, but also inhibited the regeneration processes of regenerating (amputated) worms, with LC_{10} values of 9.86 mg/L and 9.32 mg/L for the 48-h acute toxicity test, respectively. High concentration (200 mg/L) of GO killed all the worms after 3 (regenerating) or 4 (homeostasis) days of exposure. Whole-mount in situ hybridization (WISH) and immunofluorescence analyses suggest GO impaired stem cell proliferation and differentiation, and subsequently caused cell apoptosis and oxidative DNA damage during planarian regeneration. Mechanistic analysis suggests that GO disturbed the antioxidative system (enzymatic and non-enzymatic) and energy metabolism in the planarian at both molecular and genetic levels, thus causing reactive oxygen species (ROS) over accumulation and oxidative damage, including oxidative DNA damage, loss of mitochondrial membrane integrity, lack of energy supply for cell differentiation and proliferation leading to retardance of neuron regeneration. The intrinsic oxidative potential of GO contributes to the GO-induced toxicity in planarians. These data suggest that GO in aquatic systems can cause oxidative stress and neurotoxicity in planarians. Overall, regenerated tissues are more sensitive to GO toxicity than homeostatic ones, suggesting that careful handling and appropriate decisions are needed in the application of GO to achieve healing and tissue regeneration.

1. Introduction

As an oxidized form of graphene, graphene oxide (GO) has great potential applications in various fields such as healthcare (Mao et al., 2013), and environmental protection (Clemente et al., 2017). Due to its antibacterial and anti-inflammatory properties, GO has potential biomedical applications (Lu et al., 2017; Hoyle et al., 2018). It is also believed to be beneficial to tissue regeneration and wound repair (Shahnawaz Khan et al., 2015; Shang et al., 2019; Kumar et al., 2016), and is being explored as biomedicine to treat the diseases such as Alzheimer's (Meng et al., 2012), and Parkinson's disease (Xiong et al., 2020). The worldwide production, application, and disposal of GO and GO-containing nanomaterials would inevitably lead to their release into the environment (Du et al., 2017; Zhang et al., 2020), which may pose a risk to the environment and human health (Zhang et al., 2017a). The aquatic ecosystem is undoubtedly a major sink for GO in the

* Corresponding author.
** Corresponding author at: School of Geography, Earth and Environmental Sciences, University of Birmingham, Edgbaston, Birmingham B15 2TT, United Kingdom.
E-mail addresses: pangqiuxiang@sdut.edu.cn (Q. Pang), p.zhang.1@bham.ac.uk (P. Zhang).

https://doi.org/10.1016/j.ecoenv.2022.114431
Received 5 August 2022; Received in revised form 1 November 2022; Accepted 12 December 2022
Available online 13 December 2022

environment. As a result, GO can be potentially ingested by sediment-feeding benthic vertebrates (Malina et al., 2020) and invertebrates (Zhang et al., 2017b) and biomagnified in the food chain, posing a threat and risk to these animals and higher trophic level organisms.

Developing tissues and organisms are usually more sensitive to chemical exposure than mature organisms (Leynen et al., 2019; Kluever et al., 2014). In the process of rapid cell division, stem cells are vulnerable to environmental chemicals which may hinder the differentiation and development of cells (Perera and Herbstman, 2011). *In vitro* studies report contradictory results on the toxicity of GO to stem cells. For example, Zhang et al. (2010) found that few-layered graphene sheets could induce cytotoxic effects on the neural phaeochromocytoma-derived PC12 cells and that these effects are shape- and concentration-dependent. Wang et al. (2011) found that GO can enter human fibroblast cells and induce cell apoptosis with a dose > 50 mg/L. It has been suggested that the toxic effects are related to the generation of ROS caused by GO. Guo et al. (2020) reported that functionalized graphene (G-NH_2, G-OH and G-COOH) caused neurotoxicity to human neuroblastoma cells (SK-N-SH) even at 0.1 mg/L. However, contradictory results are also reported, showing that graphene-based nanomaterials can be used as a platform to support cellular attachment, differentiation, and proliferation (Li et al., 2011). For instance, Park et al. (2011) noted that a graphene scaffold increased the human neural stem cells-adhesion and differentiation by 97.4%. More studies are therefore urgently needed to understand the biological effects of graphene family materials on stem cells to address this and other controversies.

Freshwater planairans have a large number of pluripotent stem cells thus any damaged or amputated tissues including the entire central nervous system (CNS) can be regenerated, which makes them an ideal model organisms for study of the (neuro-)developmental and biomedical research (Hagstrom et al., 2016). Using the planarian model system enables us to study the influence of nanomaterials in highly dynamic stem cell systems and to promote the adoption of research strategies in line with the 3 R (reduction, replacement, and refinement of animal testing) directive (Russell and Burch, 1959). Planarians can regenerate their brains and neuro-system after amputation, allowing normal adults to be studied alongside genetically identical regenerating animals (Seifert and Muneoka, 2018). Due to this unique characteristic and the complexity of its intermediate neuronal, planarian is a good complement to the existing experimental animal models in toxicology, like nematode and zebrafish, to provide sbroader molecular toolkits (Hagstrom et al., 2015). In fact, the brain of planarian is considered to be the ancestor of vertebrate brain; the neurotransmitters and receptors are related to all major neurotransmitter systems which are found in vertebrate brain (Ofoegbu et al., 2019). Besides, the morphology and physiology of planarians' brain nervous system are similar to those of bertebrates (Ross et al., 2017).

Recently, the planarian was also established as a model for assessing nanotoxicity. For example, 200 mg/kg boron nitride NPs (a diameter of 10–80 nm and length of 10 μm) did not induce any oxidative DNA damage and cell apoptosis, and there were no adverse effects on worms stem cell biology and on *de novo* tissue regeneration (Salvetti et al., 2015), whereas 15 mg/L Ag NPs (both uncoated and PVP-coated with a nominal size of 20 nm) showed a strong interference with tissue- and neuro-regeneration of worms (Leynen et al., 2019). However, CeO_2 nanoparticles could accelerate the regeneration of planarians through scavenging wound induced ROS (Ermakov et al., 2019). A recent study exposed planarians to polystyrene micro- and nano-plastics (PS) and found that PS could delay the growth and regeneration of planarians (Gao et al., 2022). The researchers found that PS induced oxidative stress to planarians and the activation of the Notch signaling and TGFβ/SMAD4 pathways are responsible for the inhibited proliferation and differentiation of stem cells (Gao et al., 2022). Researchers often use planarians as water quality monitors in environmental research due to their high susceptibility to substances added to their environment (Rivera and Perich, 1994; Kapu and Schaeffer, 1991). After exposure to water samples, different markers at the molecular (Prá et al., 2005) or biological levels (Knakievicz, 2014) can be used to assess the water pollution level and identify specific pollutants. Since most nanomaterials, micro-and nano-plastics tend to sink to sediments after entering the aquatic system (Gao et al., 2022; Zhang et al., 2012; Little et al., 2021), planarians as benthic organisms have a high chance to absorb GO and other nanomaterials when they glide over the sediments and feed.

In this work we for first time used the freshwater planarian *Dugesia japonica* (*D. japonica*) to investigate the potential toxicity of GO nanomaterials (87 ± 4.6 nm) and the mechanisms of induced impacts on planarian stem cells, development and tissue regeneration in vivo. The (neuro-)developmental and stem cell-related effects of homeostatic (normal) planarians were explored versus regenerating (amputated) planarians. Oxidative stress responses, migration and proliferation of stem cells, and regeneration processes such as the development of head and lateral branches of neuronal cells were evaluated to explore the toxicity mechanisms of GO.

2. Materials and methods

2.1. Chemicals and animals

GO was purchased from Chengdu Organic Chemicals Co. Ltd. (Chengdu, China). Details of morphology, lateral size and thickness, chemical structure, ζ-potential, and hydrodynamic sizes of GO are described in the supporting information (**SI**, **Section I**). All other commercial chemicals were purchased from Sigma-Aldrich. The model animal, freshwater planarian *Dugesia japonica*, was established in our lab. The detailed planarian cultivation was described in **SI**.

2.2. Phenotype and post-exposure locomotion velocity (pLMV) assays

Thirty planarian *(D. japonica)* were exposed for 7 days to a series (0, 1, 10, 20, 50, 100, and 200 mg/L) of GO suspensions prepared in MW medium. The number of live worms was recorded every day. The growth of the regeneration bud (blastema) was evaluated by measuring the size using computer morphometry as described previously (Ermakov et al., 2019). The worms were photographed with a Nikon SMZ 1500 stereomicroscope (Nikon, Japan) at 2, 3, 4, 5, 6, and 7 dpa, i.e., after the decapitation. The area of the blastema and the total area of the body were determined using Image J software (Version 1.8.0, Wayne Rasband, National Institutes of Health, Bethesda, MD, USA). The detailed experimental design was described in **SI** (Fig. S1).

In each treatment, thirty worms were placed in a clear acrylic box (50.0 cm by 50.0 cm) placed over graph paper (grid lines spaced 0.5 cm apart) with MW medium underneath. Usually, 5 ~ 8 min is recommended for a *pLMV* test (Raffa and Valdez, 2001; Zhang et al., 2013), therefore, we observed the behavior of planarian in 8 min. The observation started 30 s after placement of the planarians at the center of the grid and lasted for 8 min. The planarian's *PLMV* was determined by the number of grid lines that the worm crossed or recrossed over an observation period of 8 min.

2.3. Oxidative stress responses

The ROS accumulation in the cells of the worms was determined after dissociation treatment following the method described previously (Pirotte et al., 2015) with a minor modification (details are provided in the **SI**). Briefly, we rinsed the dissociated cells with deionized water (DI water) and immersed them in PBS buffer (pH 7.4) containing 10 μM 2′, 7′-dichlorodihydrofluorescein diacetate (DCFH-DA) solution for 20 min, and then rinsed with PBS buffer followed by measurement at Ex/Em 485 nm/528 nm using a Thermo Varioskan Flash (Thermo Fisher

Scientific, USA). The ROS in the whole body was also visualized (Details are presented in the **SI**).

To analyze the antioxidative enzymes and lipid membrane integrity, the supernatant was collected for analysis. SOD, POD, CAT, GPx, GST and GR activities, and MDA contents were determined as per the manufacturer's instructions in the assay kits (Nanjing Jiancheng Bioengineering Institute, Nanjing, China). Assay kits were also used to measure non-enzymatic anoxidant levels in GSH and GSSG (Beyotime Institute of Biotechnology, Shanghai, China). Details of the analyses are provided in the **SI**.

2.4. Mitochondrial integrity and adenosine triphosphate (ATP)

Mitochondria were isolated following the method described previously (Yuan et al., 2016). Mitochondrial membrane integrity was measured using a JC-1 assay kit (Beyotime Biotech, Nantong, China) as per the manufacturer's protocol. The ATP content and total ATPase activity were measured using an Enhanced ATP Assay Kit (Beyotime Institute of Biotechnology) and an ATP assay kit (Nanjing Jiancheng Bioengineering Institute), respectively, using a Thermo Varioskan Flash (Thermo Fisher Scientific, USA). A Bicinchoninic Acid Protein Assay kit (BCA, Thermo Fisher Scientific, Waltham, MA) was used to measure the protein concentration.

2.5. Real-time quantitative PCR analysis

Differential expression of oxidative stress-associated genes (*gpx*, *gr*, *gst,* and *nak*) in worms were detected using quantitative real-time PCR (qPCR) after exposure to GO (50 mg/L) for 48 h. The primer sequences are provided in Table S1 in the supplemental information (**SI**). Based on the manufacturer's protocol, an SYBR Real-time PCR mixture (BioTeke, China) was used for qPCR analyses using a LightCycler 480 II Real-Time PCR System (Roche, Basel, Switzerland). The detailed method is shown in the **SI**.

2.6. Whole-mount in situ hybridization (WISH) and immunofluorescene

After 2 days of exposure to GO (50 mg/L), the intact and regenerated worms (2 days after amputation) were used for in situ hybridizations. The experiments were performed to characterize the expression level of *Djpiwi-A*, a stem cell marker gene (Shibata et al., 2010) following a previously described method (Gao et al., 2021). The worms were prepared for immunochemistry following a previously described method by Dong et al. (2019). Details of the experiments are shown in the **SI**.

2.7. ELISA for Caspase-3 and 8-OHdG activities

Cleaved cysteine-aspartic proteases-3 (caspase-3), an apoptotic marker, was quantified in worm's tissue using a commercially available ELISA assay (Jiangsu Jingmei Biotechnology Co., Ltd, Jiangsu, China). To measure DNA oxidative damage, we used a DNA Damage ELISA kit (Jiangsu Jingmei Biotechnology Co., Ltd, Jiangsu, China) to detect 8-hydroxy-2 deoxyguanosine (8-OHdG) content. All assays followed the protocols supplied by the manufacturer. Details of sample preparation and the analyses are shown in the **SI**.

2.8. Oxidative potential of GO by a GSH oxidation assay

The intrinsic oxidative potential of GO was evaluated using Ellman's reagent as described previously with a minor modification (Xie et al., 2020). A spectrophotometric method was conducted to quantify non-oxidized GSH using Ellman's reagent (5, 5′-dithiobis (2-nitrobenzoic acid), DTNB), which reacts with GSH thiol groups to form 3-thio-6-nitrobenzoate (TNB). Details of the experiments are shown in the **SI**.

2.9. Statistical analysis

Data are expressed as mean ± SD (standard deviation) after three repetitions of each tests. Student's t-test or ANOVA was used to examine statistical significance. A significant level was defined as $p < 0.05$.

3. Results and discussion

3.1. Characterization of GO

As shown in Fig. S2, FT-IR spectra shows that GO had a large amount of oxygen-containing groups (C-O group at 1416 and 1052 cm^{-1}, C═O group at 1726 cm^{-1}, O-H group at 3400 cm^{-1}). The I_D/I_G value was lower than 1 in the Raman spectrum, suggesting slight defects in the GO structure. The average lateral size of the GO was 87 ± 4.6 nm and the thickness was 0.83 ± 0.24 nm, as revealed by AFM. DLS analysis shows that the GO had a negative charge in DI water and mineral water (MW). The hydrodynamic diameter of GO in the worm's mucus medium was 1678 ± 97 nm, which was larger than that in MW (1394 ± 72 nm) and DI water (1054 ± 49 nm) (Table S3). The high salinity and the excretion of organic material by planarian into the mucus medium could compress the double electric layer on the surface of the GO nanomaterials, resulting in strong aggregation (Zhang et al., 2020).

3.2. GO exposure caused acute toxicity and inhibition of mobility in homeostatic planarian

As shown in Fig. S3a, GO induced acute toxicity in a time- and dose-dependent manner. GO at 10 mg/L inhibited the survival rate by 10% at 2 d and 16.7% at 7 d of exposure. GO exposure at 200 mg/L caused the highest toxicity, killing all the worms at 4d after exposure. The 1, 2, 3, 4, 5, 6, and 7 d LC_{50} values of GO for homeostatic worms were 153.5 mg/L, 133.2 mg/L, 107.4 mg/L, 95.8 mg/L, 93.5 mg/L, 88.7 mg/L, and 81.2 mg/L, respectively (Fig. S3a), suggesting increased toxicity over time. Similarly, GO also reduced the mobility of the worms in a time- and dose-dependent manner (Fig. S3b). Before death, growth and reproduction, behavior is normally altered. In fact, the latter is more sensitive than mortality as a biomarker (Alonso and Camargo, 2011; Beketov and Liess, 2008). We examined the mobility using *PLMV* test, which is a convenient and sensitive metric to quantify planarian behavioral responses (Raffa and Valdez, 2001). In this study, data were plotted as cumulative means over 8 min for each group.The slope of the plot represents the speed of movement across the gridlines. The worms in the control groups (CT) displayed an average *pLMV* of about 20–25 gridlines per minute (the slope value is 21.5). We observed the mobility again after 2 days of exposure. GO started to inhibit the mobility of the worms from the concentration 10 mg/L, with the *pLMV* reduced by 35.8% compared to the CT group. GO at 20, 50, and 100 mg/L reduced the slope of the *pLMV* to 11.3, 6.5 and 3.6, respectively. The change of behavior induced by GO exposure are most likely caused by its neurotoxic action since the behavior is highly dependent on neuronal activity (Inoue et al., 2015). GO has also been reported to be neurotoxic in different biological models, including SH-SY5Y (Lv et al., 2012), zebrafish (Hu et al., 2017), and *Caenorhabditis elegans (*Li et al., 2017*)*. Together, the dose- and time-dependent neurotoxicity suggest that GO showed acute neurotoxicity to the planarian tested.

3.3. GO impedance of the tissue regeneration of planarian

Once lose part of its body, neoblast cells would migrate to wound sites, proliferate, and differentiate to form new tissues and organs in planarians (Pellettieri et al., 2010). Previous studies showed that the neoblast proliferation and differentiation are affected by environmental factors such as contaminants (Leynen et al., 2019; Dong et al., 2021). Therefore, we also checked the impact of GO on the neuro-developmental process and examined the proliferation and

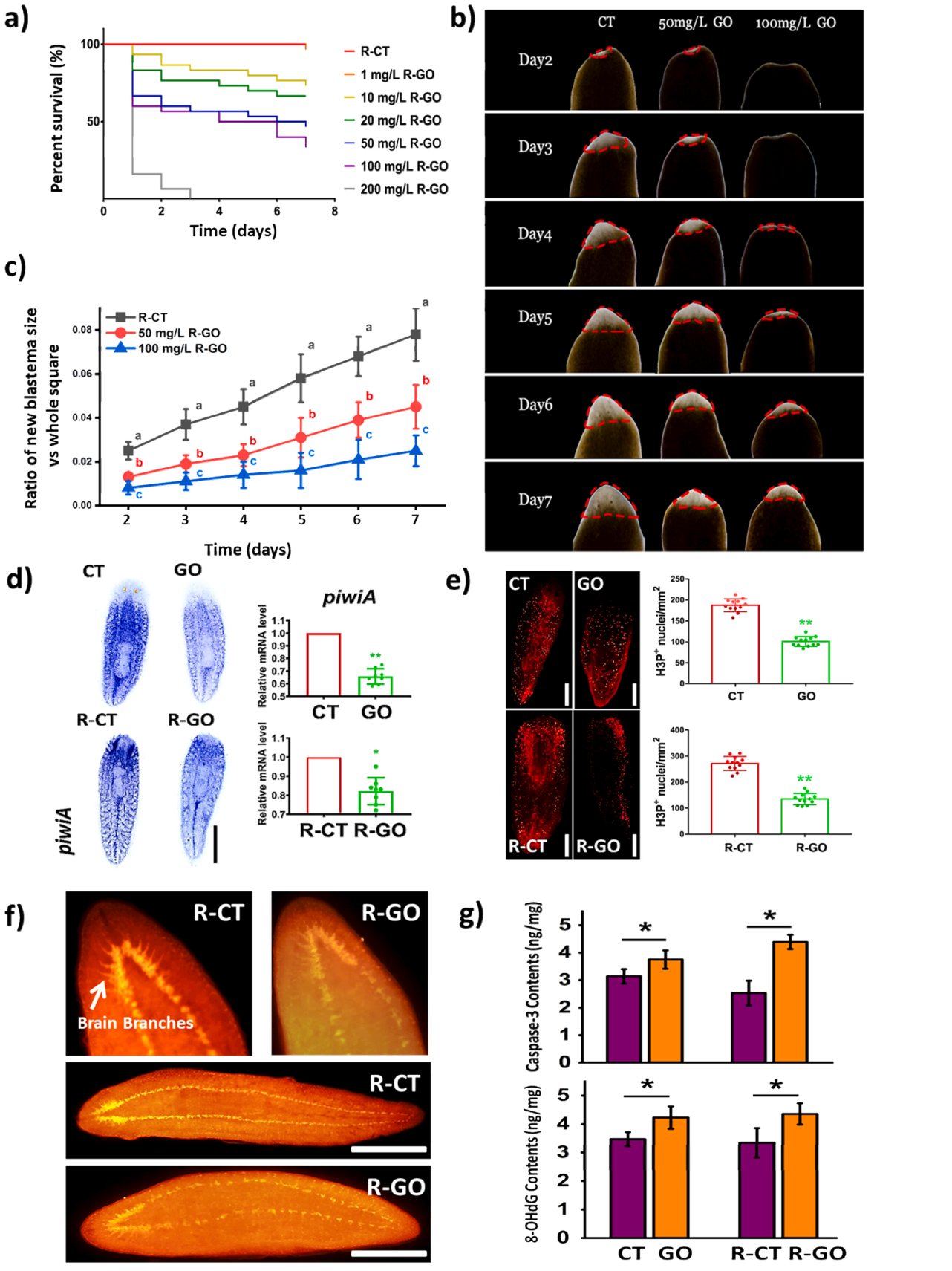

(caption on next page)

Fig. 1. Impacts of GO on tissue regeneration and stem cells preliferation. **(a)** Survival of regeneration worms after GO exposure. **(b)** Microphotographs of new blastema after 7 days of exposure to 50 and 100 mg/L of GO. **(c)** Area ratio of new blastema to the whole-body square (Fig. S5). (**d**) Left, in situ hybridization to detect *DjpiwiA* transcripts in worms. Right, the expression of *DjpiwiA* was reduced in the homeostatic and regeneration worms after exposure to 50 mg/L GO. (**e**) Immunohistochemistry using the mitotic marker Anti-H_3P antibody. The left panel shows a view of the homeostatic worm and the head regeneration of control and GO treatments. Right, the number of mitotic events in GO treatment and CT groups. Whole-mount immunostaining of the nervous system with anti-SYNORF1 (3C11) in regeneration worms after exposure to 50 mg/L GO for 10 days (**f**). Contents of caspase-3 (**f**, upper) and 8-OHdG (**f**, lower) in homeostatic and regeneration worms affected by GO treatments. * and the different letters indicates a significant difference at $p < 0.05$ compared with the corresponding control. The results are presented as the mean ± SD of a minimum of 6 biological replicates. Scale bar: 1 mm. R stands for regeneration.

apoptosis of regenerating fragments.

Similar to the homeostatic worms, the survival rates of regeneration worms were also reduced by GO in a time and dose-dependent manner, while the effects were stronger than on the homeostatic worms. The LC_{50} of GO to the regeneration worms were 113.4 mg/L, 101.8 mg/L, 94.1 mg/L, 80.3 mg/L, 65.1 mg/L, 57.2 mg/L and 51.8 mg/L, respectively at 1, 2, 3, 4, 5, 6, and 7 dpa (Fig. 1**a**). The survival rate was reduced by 13.4% and 26.7% respectively after 2 and 7 days of exposure to 10 mg/L GO. The rate was dramatically reduced by 200 mg/L GO, with only 16.1% survival at 1 d post-exposure and all had died after 3 d of exposure. Fig. S4 shows that a high concentration (100 mg/L) of GO caused necrotic lesions and lysis of the tissues, which led to death eventually.

We further examined the effect of GO exposure on tissue regeneration by measuring the size of the newly growing blastema. Based on the LC_{50}, we used 50 or 100 mg/L for the subsequent studies. As shown in Fig. 1**b**, the anterior blastema sizes in the GO-exposed planarian were significantly smaller compared with those in the CT group (Fig. 1**b**). The blastema was visible only until 4d after exposure to 100 mg/L GO, suggesting retardation of tissue regeneration. The quantitative analysis (Fig. 1**c**) showed that the blastema sizes were 42.3% and 67.9% smaller in the 50 mg/L and 100 mg/L GO treatments, compared with the size in the CT at 7 dpa. Tissue regeneration relies on stem cells proliferation, migration, and differentiation especially, thus a significant decrease in stem cell proliferation underlies the disturbed regeneration process (Barghouth et al., 2019). We therefore explored the underlying mechanism by examining the impacts of GO on stem cells at the molecular level.

3.4. GO impaired stem cell dynamics and regeneration of the nervous system

DjpiwiA, a main gene marker for stem cells, was examined using WISH to characterize its expression level (Dong et al., 2021). For the homeostatic worms, *DjpiwiA* was extensively expressed (shown as a blue color) in the whole body except for the pharynx and head (Fig. 1**d**), and the expression was reduced by 34.3% after 2 days of exposure to 50 mg/L GO. The head was fully regenerated 7 d after amputation in the R-CT group, evidenced by the strong expression of *DjpiwiA*. Again, GO exposure impaired the regeneration as shown by the 17.9% lower expression of stem cells at 2 dpa.

Mitotic activity was examined in vivo by labeling stem cells' nuclei with an anti-phospho-Histone H3 antibody. Compared with the CT group, the number of nuclei significantly decreased (by 46.3%) after GO treatment (Fig. 1**e**), suggesting impaired cell proliferation. In the process of regeneration (R-CT), the cell proliferation was accelerated for tissue regeneration, as compared with the CT group. However, the cell proliferation was severely inhibited by the GO treatment, with the number of nuclei reduced by 50.3% compared to the CT. The planarian brain contains several thousands of neurons, which can be fully regenerated *de novo* after injury through the stem cells. Previous studies have indicated that GO may be unable to guide neural growth but may facilitate regaining tissue integrity after spinal cord injury (López-Dolado et al., 2015). GO was also found to induce intracellular redox deviation, and autophagy-lysosomal network dysfunction leading to disrupted mitochondrial homeostasis in human Y5Y neuroblastoma cells (Xiaoli et al., 2021). To evaluate whether the reduced stem cell activity caused by GO further impacted the regeneration of the nervous system, the neuron morphologies were observed after 10 days of exposure to GO using a whole-mount immunofluorescence assay. The anti-SYNORF1 antibody was used as a biomarker, which allows visualization of the planarian CNS. Planarian brains have an inverted U-shaped structure composed of neural cells and axons displaying rich branching (Umesono et al., 1999). We found that GO treatment significantly reduced the density of nerve fibers and the number of lateral branches (Fig. 1f and Fig. S6). These results revealed that GO induced neural regeneration defects in the treated worms, which manifested as a decreased number of neuronal cells and decreased lateral branches compared to CT (Fig. 1**f**). In fact, GO accumulation and biodistribution in the regeneration tissues and organs may cause a direct toxicity (Chatterjee et al., 2017). Similarly, Kim et al. (2018) also used Raman spectroscopy to analysis the in vivo uptake GO in *Caenorhabditis elegans* (*C. elegans*). They found that GO were deposited in the pharynx and the intestine, which further supported the strong reproductive toxic potential of GO in *C. elegans (*Kim et al., 2018*)*. Ma et al. (2015) found that larger GO showed a stronger adsorption onto the plasma membrane which may enhance production of inflammatory cytokines and small GO sheets were more likely taken up by cells. Overall, these results correlated with each other, suggesting that GO exposure impaired the stem cell activity and thus the health and regeneration capacity of the CNS in the exposed worms. Further experiments at the molecular level suggest that GO exposure induced higher cell apoptosis and DNA damage (Fig. 1**g**). DNA damage caused by GO exposure was also reported in other models, e.g., MDA-MB-231 human breast cancer cells, where DNA mutagenesis occurred (Liu et al., 2013). A previous study also suggested that GO caused chromosomal aberrations and DNA fragmentation of stem cells at ppm levels (Akhavan et al., 2013). Since 8-OHdG is a maker for oxidative DNA damage, the increase of 8-OHdG indicates an oxidative stress induced DNA damage, which may contribute to the reduced mitosis (Fig. 1**e**). To further demonstrate this hypothesis and the underlying toxic mechanism, we next analyzed the responses of the antioxidative system in the worms following GO exposure.

3.5. GO exposure induced disruption of the antioxidant system

Overproduction generation of ROS is one of the most important mechanisms of toxicity induced by nanomaterials (Seabra et al., 2014). While scavenging of ROS is also a mechanism for the protective effects induced by some nanomaterials such as CeO_2 (Ermakov et al., 2019). Therefore, ROS level, e.g., the redox balance, is an important indicator for nanomaterial induced biological effects. We first detected changes in the intracellular ROS levels in the planarian cells 2 days post-exposure to GO. As shown in Fig. S7, the intracellular ROS levels in homeostatic and regeneration worms were significantly enhanced by 160% and 180%, respectively, relative to the control following GO treatment. The ROS levels in the whole body were also examined (Fig. S8), and again the ROS levels were higher after GO treatments compared with the CT or R-CT. In fact, the physicochemical properties of nanomaterials, such as shape, size, surface chemistry and the degree of aggregation influence the production of free radicals and subsequent oxidative stress (Aillon et al., 2009). The aggregation of nanomaterials is a key factor leading to the apparent controversies on the toxic mechanism of nanomaterials in literature. Generally speaking, the harmfulness of NPs may arise from their size-related ability to readily enter biological system (Lovrić et al., 2005). Many studies also demonstrated NPs aggregation changes the

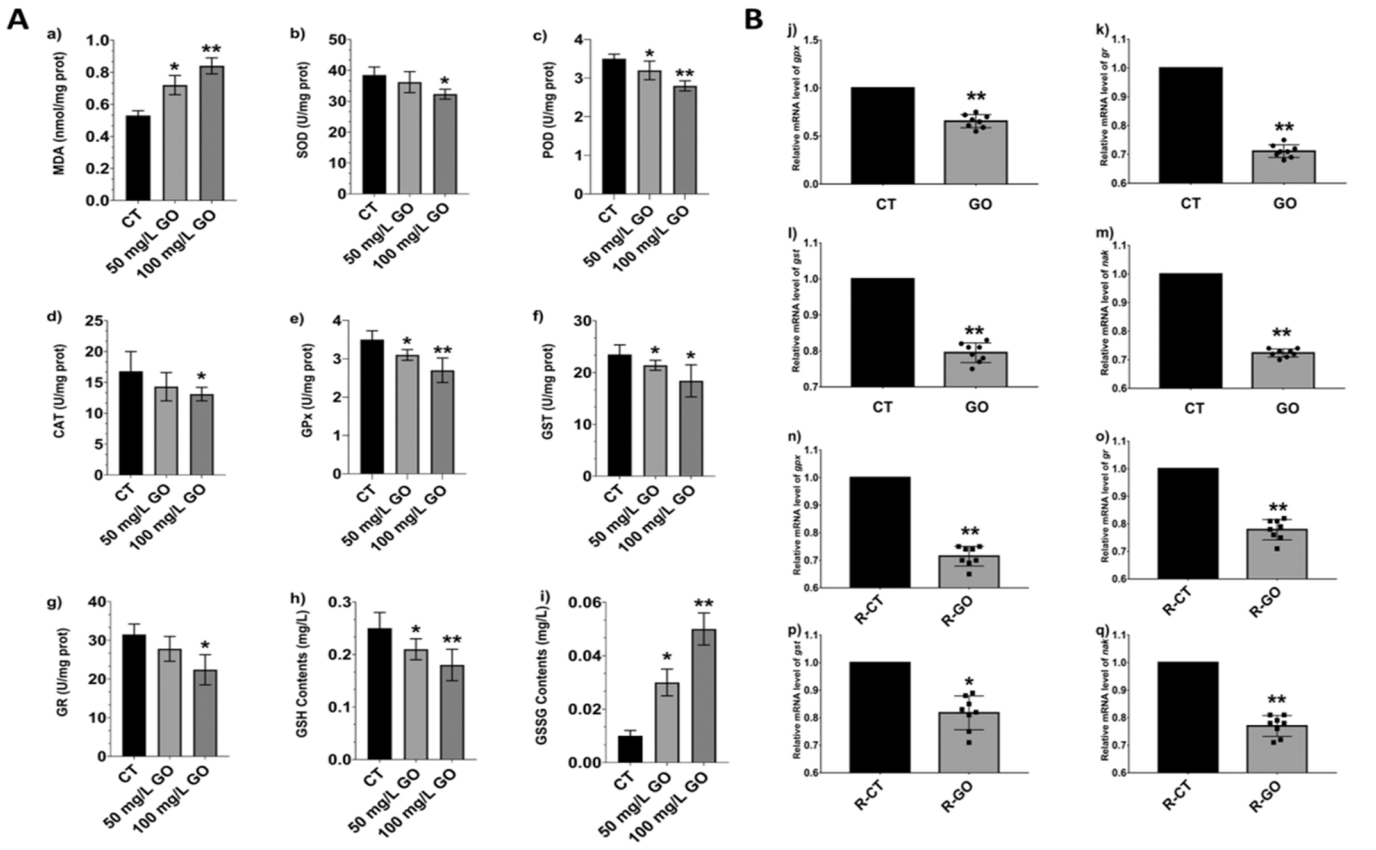

Fig. 2. Alteration of antioxidant markers and oxidative stress-related genes expression. Left (A), MDA (**a**), SOD (**b**), POD (**c**), CAT (**d**), GPx (**e**), GST (**f**), GR (**g**), GSH (**h**) and GSSG (**i**) contents in homeostatic worms after exposure to GO for 48-h. **Right (B)**, the effect of GO on relative mRNA expression levels of gene *gpx*, *gr*, *gst*, and *nak* was measured in homeostatic worms (**j**, **k**, **l**, and **m**) and regeneration worms (**n**, **o**, **p**, and **q**) exposed for 48-h. * $p < 0.05$ and * * $p < 0.01$ indicate differences as compared to the control group (CT). R stands for regeneration.

retention time of particles which may increase or decrease the toxicity (Murugadoss et al., 2020). Most studies observed that as the particle size decreases, there is a tendency for toxicity to increase, even if the same material is relatively inert in a bulkier form (Sharifi et al., 2012). Herein, in this study we believed that GO aggregation may decrease its nanotoxicity due to the original size of material only 80 nm which needs further study to demonstrate this hypothesis.

High levels of ROS may lead to a string of adverse consequences such as damage to membrane integrity, DNA, protein, or subcellular structures. Indeed, DNA damage has been demonstrated above (Fig. 1**g**). Loss of membrane integrity is also considered to be a marker of cytotoxicity induced by nanomaterials (Hashemi et al., 2016). Similarly, Ma et al. (2021a). found benzo[*a*]pyrene-bearing fine biochar particles elicited a severe disruption of the phospholipid membrane and oxidative stress. The membrane integrity was impaired as shown by the increased MDA levels (Fig. 2**a**) which is a marker of lipid membrane oxidation. To cope with the excessive ROS in the body, the antioxidant defense system including enzymatic (SOD, POD, CAT, GPx, GST) and non-enzymatic (GSH-GSSG) processes can be triggered. These compounds work synergistically to protect organisms from ROS-induced oxidative damage. Our results showed that the activities of both enzymatic and non-enzymatic antioxidants were down-regulated in both homeostatic (Fig. 2**A**) and regeneration worms (Fig. S9), thus causing the inability of the worms to eliminate the excessive ROS and driving the consequent oxidative damage. Specifically, POD, GPx, and GST activities significantly decreased in all GO-treated groups (Fig. 2**c**, **e**, and **f**, $p < 0.05$). SOD, CAT, and GR activities were reduced significantly only in the 100 mg/L GO treatment (Fig. 2**b**, **d**, and **g**, $p < 0.05$). A similar pattern of impacts on the non-enzymatic antioxidant system was also observed (Fig. 2**h and i, and** Fig. S8). The GSH contents decreased by 16.1% and 28.2% after exposure to 50 and 100 mg/L GO for 2 d, compared with CT. In regeneration worms, the GSH content decreased by 22.6% and 32.3% at 2 dpa, respectively. Correspondingly, a significant increase of the GSSG content, an oxidized form of GSH, was observed in both types of worms (homeostatic and regenerative) after exposure to GO.

We further examined whether the antioxidant system was impaired at the genetic level by examining the mRNA expression of some key genes including GPx gene (*gpx*), GR gene (*gr*), GST gene (*gst*) that control antioxidant production and the Na^+/K^+-ATPase gene (*nak*) which is responsible for ATP synthesis, using the qRT-PCR technique. As shown in Fig. 2**j-q**, *gpx*, *gr*, *gst*, and *nak* expressions were significantly down-regulated after 2 days of exposure to GO. Similar patterns were also observed in the regeneration worms (Fig. 2**B**). The results above suggest that GO exposure impaired the antioxidant systems in the worms at both genetic and molecular levels, thus causing the accumulation of excessive ROS in their bodies and subsequent oxidative damage.

3.6. GO disruption of energy metabolism

Energy is essential for biota and is especially critical for the nervous system which consumes 20% of the total energy produced by the body to maintain its normal function (Pulido and Ryan, 2021). To further understand the mechanism of GO-induced impairment of the growth and tissue regeneration in planarians, we examined the ATP level, the ATPase level, and the mitochondria membrane integrity which is where the energy is produced. Previous studies have indicated that GO may affect mitochondrial function and change the energy metabolism in A549 tumor cells and SH-SY5Y cells (Xiaoli et al., 2021; Zhang et al., 2019). When mitochondrial energy is depleted, intracellular ion pumps that rely on ATP may face a variety of transport barriers. ATP synthesis is

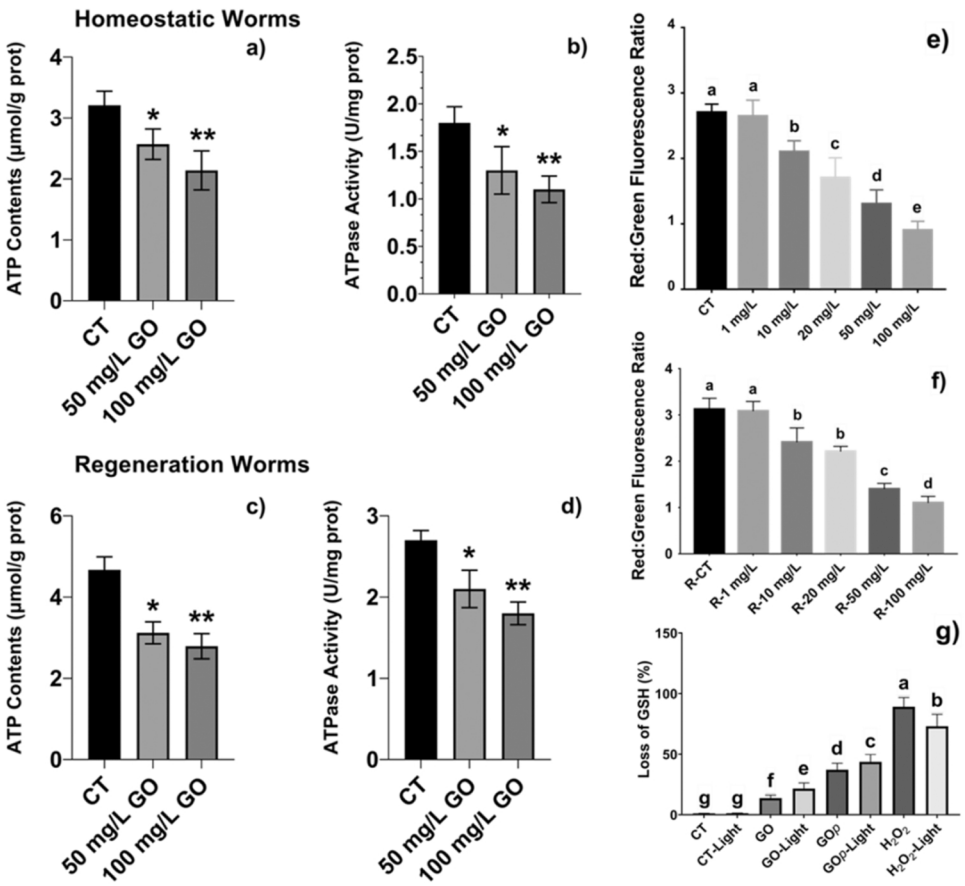

Fig. 3. GO disrupted the mitochondrial function. Effects of exposure to 0, 50 and 100 mg/L GO on ATP contents (**a**) and ATPase activity (**b**) in homeostatic worms, and ATP contents (**c**) and ATPase activity (**d**) in regeneration worms exposed for 48-h. * $p < 0.05$, * * $p < 0.01$. Effect of the different concentrations of GO on the mitochondrial membrane potential (MMP) of homeostatic (**e**) and regeneration worms (**f**). Percentage of GSH loss (**g**) due to oxidation by GO and GO*p* with or without light for 3 h. Different letters indicate significant difference. R stands for regeneration.

impaired when mitochondrial ion transport is dysfunctional. A dysfunctional ion transport system can generate intracellular free radicals, which damage cytoplasmic membranes (Kourie, 1998). As shown in Fig. 3**a** and **c**, ATP content significantly decreased in GO groups compared with CT ($p < 0.05$) in both homeostatic and regeneration worms. The activity of ATPase was reduced by 27.8% and 38.9%, and 22.2% and 33.3% in homeostatic and regeneration worms, respectively, following 50 and 100 mg/L GO treatment (Fig. 3**b** and **d**). ATPase, a protease on bio-membranes, plays a vital role in material transport, energy conversion, and information transmission. The activity of ATPase is thus an important index for evaluating energy metabolism and cell functions (Serrano, 1989).

The reduction in ATPase activity can occur when the lipid membranes undergo oxidative damage (Figs. 2**a**, 3**a,** and **c**). Duch, et al (Duch et al., 2011). reported that GO could induce cytotoxicity toward alveolar epithelial cells and macrophages through ROS generation, causing impaired mitochondrial respiration and cell apoptosis. A recent study also found that GO can disrupt mitochondrial homeostasis by inducing intracellular redox deviation, which eventually leads to apoptotic death (Xiaoli et al., 2021). Mitochondrial dysfunction can affect the balance of extracellular and intracellular ROS levels, thus causing further oxidative damage (Lim et al., 2007). The mitochondrial membrane integrity was analyzed by measuring the mitochondrial membrane potential (MMP), the decrease of which is a crucial indicator of mitochondrial dysfunction. As shown in Fig. 3**e** and **f**, the MMP was significantly reduced after GO exposure, as shown by the ratio of red to green fluorescence intensity. In the homeostatic group, the MMP decreased by 51.8% and 66.7% compared to the CT, respectively, following 50 mg/L and 100 mg/L GO exposure. Likewise, in regeneration worms, the MMP decreased by 55.1% and 64.7%, respectively. Graphene-based nanomaterials could trigger mitochondrial pathways, activate caspase-3, and eventually cause cell apoptosis (Li et al., 2012). Excessive ROS in mitochondria could cause the loss of MMP and thus disrupt the electron transport chain and energy metabolism (Guo et al., 2020). Few-layer graphene could also induce the increase of Ca^{2+} level in cytoplasmic, which results in the depolarization of the mitochondrial membrane, increased membrane permeability and apoptosis (Sasidharan et al., 2016). Our results agree with these previous reports, and demonstrate that GO-induced failure of the antioxidant system and the resultant ROS over-accumulation contributed to the impaired mitochondrial function and energy metabolism, and cellular apoptosis.

3.7. *Chemical origin of the toxicity: the intrinsic oxidative potential of GO*

GO may have intrinsic oxidative potential (Pieper et al., 2016) which can oxidize intracellular antioxidants (e.g. GSH), thereby reducing the antioxidative capacity of the cells (Ma et al., 2021b). We thus examined the oxidative potential of GO using an in vitro GSH oxidation assay (Xie et al., 2020). Since the exposure experiments were performed under a light/dark cycle, the oxidative potential under both dark and light conditions was examined. As shown in Fig. 3**g**, 13.8% and 21.7% of GSH were lost after incubation with pristine GO under dark and sunlight conditions, respectively. This suggests that GO has an intrinsic oxidative potential and that GO can cause stronger oxidation under light exposure, which might be due to the photo-enhanced electron transfer and generation of electron holes that enhance GSH oxidation (Chong et al., 2017). GSH oxidation can cause depletion of GSH in the body leading to reduced antioxidant capacity and failure of the planarian to protect themselves from ROS attack. GSH oxidation partly relies on a direct chemical reaction between the GO surface and GSH molecules. However, in biological surroundings, e.g. in the planarian culture medium, the biomolecules (e.g., mucus) secreted by the worms may form a bio-corona layer on the GO surface, which may change their oxidative potential. To examine this possibility, we also collected the GO after

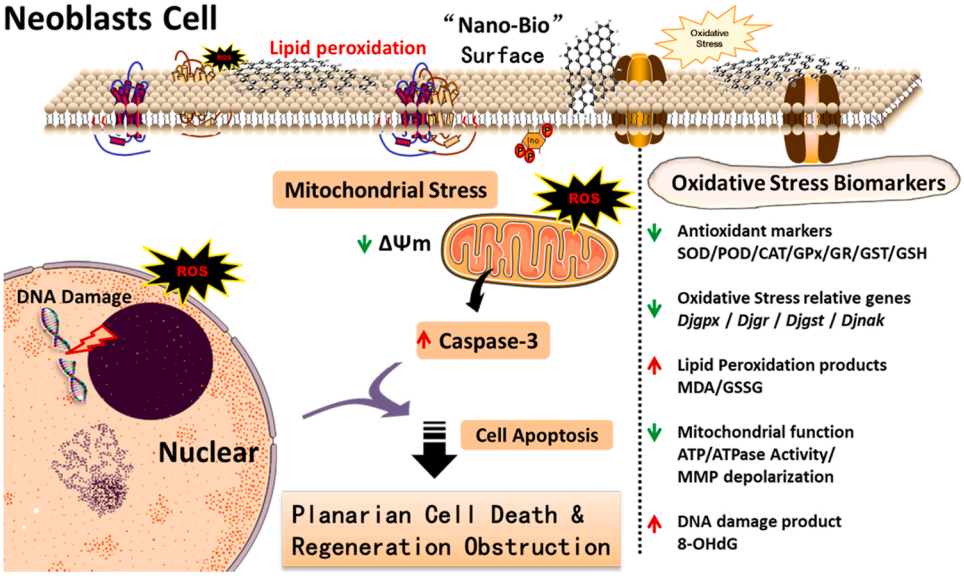

Fig. 4. Schematic model for the mechanism of GO influenced planarian cell death and obstruction of regeneration processes. GO interacted with the cell membrane, triggering lipid peroxidation by inducing ROS generation. GO-derived ROS impaired mitochondrial homeostasis and induced a significant decrease of mitochondrial membrane permeability (Δψm) such that the functioning of the mitochondria was lost. The intracellular redox loop is broken, and the sequential cellular responses exacerbated mitochondrial stress, which caused DNA damage and apoptotic cell death. Therefore, the proliferation, migration, and differentiation of neoblast cells are obstructed, which leads to the failure of the regeneration process eventually.

incubation with the worms (GO_p) and determined their GSH oxidation capacity. We found that GO_p showed significantly stronger oxidative potential than the pristine GO (37.2% and 43.7% higher in dark and light conditions when compared with untreated controls, respectively). This interaction with secreted mucus may explain the enhanced toxicity (decreased LC_{50}) of the GO to the planarian with extended exposure time. It should be noted that the intrinsic oxidative potential of GO is highly related to its physicochemical properties such as lateral size and surface chemistry. Therefore, the results presented here only represent the unique GO in this study. GO characteristics need to be studied in future to determine their neurotoxicity. For example, GO with higher surface oxygen content may has higher GSH oxidation capacity thus is expected to have higher neurotoxicity to planarian. Actually, the passage of exogeneous fine particles and nanomaterials into the animals brain may cause a harmful effects on the central nervous system and then induce neurotoxicity. Qi et al. (2022) used isotope labeling technology to obtain evidence that exogeneous particles into the CNS and their transport into the brain tissues. Isotope labeling technology may help us to track the passage of GO into planarian body from pharynx and the intestine and then transport to the blastema (new brain), which may provide additional insights for the negative effects of GO on the brain and the development of neurological system. Further studies quantifying the uptake of GO in planarian are thus necessary in the future.

4. Conclusions

In summary, a freshwater planarian's homeostasis and tissue regeneration were impaired by GO for the first time in this study. The pathways of GO-induced impairment of tissue regeneration are shown in Fig. 4. The intrinsic oxidative potential of GO caused oxidative damage to the stem cell proliferation and differentiation and thus obstructed the regeneration and development of the neuron system. This study suggests that GO may also have a significant negative effect on aquatic organisms and thus the overall ecosystem health. Our findings also provide important data regarding the impacts of GO on neurodevelopment and regeneration toxicology and highlight the need for ongoing and extensive safety evaluation of GO. A balance between GO's efficacy and toxicity is necessary to ensure its future industry applications, as well as its potential impact on ecosystems and human health.

CRediT authorship contribution statement

Changjian Xie: Conceptualization, Methodology, Investigation, Formal analysis, Writing-original draft, Funding acquisition. **Xiaowei Li:** Methodology, Resources. **Zhiling Guo:** Resources, review & editing. **Yuling Dong:** Investigation, Funding acquisition. **Shujing Zhang:** Resources. **Ao Li:** Resources. **Shan Ma:** Investigation. **Jianing Xu:** Formal analysis, Funding acquisition. **Qiuxiang Pang:** Resources. **Willie J.G. M. Peijnenburg:** writing, review & editing. **Iseult Lynch:** Funding acquisition, Writing-review & editing. **Peng Zhang:** Conceptualization, Methodology, Formal analysis, Writing-review & editing, Resources.

Declaration of Competing Interest

The authors declare that they have no known competing financial interests or personal relationships that could have appeared to influence the work reported in this paper.

Data availability

No data was used for the research described in the article.

Acknowledgments

This work was supported by the National Natural Science Foundation of China (Grant Nos. 12105163, 32001987) and the Natural Science Foundation of Shandong Province (Grant Nos. ZR2020QD133, ZR2020QC241, ZR2020MC142). Additional support from H2020 project NanoCommons (Grant Agreement No. 731032) and NanoSolveIT (Grant Agreement 814572) are acknowledged. Funding supports from the Royal Society International Exchange Programs (1853690 and 2122860) are also acknowledged.

Appendix A. Supporting information

Supplementary data associated with this article can be found in the online version at doi:10.1016/j.ecoenv.2022.114431.

References

Aillon, K.L., Xie, Y., El-Gendy, N., Berkland, C.J., Forrest, M.L., 2009. Effects of nanomaterial physicochemical properties on in vivo toxicity. Adv. Drug Deliv. Rev. 61 (6), 457–466.
Akhavan, O., Ghaderi, E., Emamy, H., Akhavan, F., 2013. Genotoxicity of graphene nanoribbons in human mesenchymal stem cells. Carbon 54, 419–431.
Alonso, Á., Camargo, J.A., 2011. The freshwater planarian Polycelis felina as a sensitive species to assess the long-term toxicity of ammonia. Chemosphere 84 (5), 533–537.

Barghouth, P.G., Thiruvalluvan, M., LeGro, M., Oviedo, N.J., 2019. In *DNA damage and tissue repair: What we can learn from planaria*. Seminars in cell & developmental biology, 2019. Elsevier,, pp. 145–159.
Beketov, M.A., Liess, M., 2008. Potential of 11 pesticides to initiate downstream drift of stream macroinvertebrates. Arch. Environ. Contam. Toxicol. 55 (2), 247–253.
Chatterjee, N., Kim, Y., Yang, J., Roca, C.P., Joo, S.-W., Choi, J., 2017. A systems toxicology approach reveals the Wnt-MAPK crosstalk pathway mediated reproductive failure in Caenorhabditis elegans exposed to graphene oxide (GO) but not to reduced graphene oxide. (rGO).Nanotoxicology 11 (1), 76–86.
Chong, Y., Ge, C., Fang, G., Wu, R., Zhang, H., Chai, Z., Chen, C., Yin, J.-J., 2017. Light-enhanced antibacterial activity of graphene oxide, mainly via accelerated electron transfer. Environ. Sci. Technol. 51 (17), 10154–10161.
Clemente, Z., Castro, V.L.S., Franqui, L.S., Silva, C.A., Martinez, D.S.T., 2017. Nanotoxicity of graphene oxide: Assessing the influence of oxidation debris in the presence of humic acid. Environ. Pollut. 225, 118–128.
Dong, Z., Cheng, F., Yang, Y., Zhang, F., Chen, G., Liu, D., 2019. Expression and functional analysis of flotillins in Dugesia japonica. Exp. Cell Res. 374 (1), 76–84.
Dong, Z., Huo, J., Liang, A., Chen, J., Chen, G., Liu, D., 2021. Gamma-Secretase Inhibitor (DAPT), a potential therapeutic target drug, caused neurotoxicity in planarian regeneration by inhibiting Notch signaling pathway. Sci. Total Environ. 781, 146735.
Du, T., Adeleye, A.S., Keller, A.A., Wu, Z., Han, W., Wang, Y., Zhang, C., Li, Y., 2017. Photochlorination-induced transformation of graphene oxide: Mechanism and environmental fate. Water Res. 124 (1), 372–380.
Duch, M.C., Budinger, G.R.S., Liang, Y.T., Soberanes, S., Urich, D., Chiarella, S.E., Campochiaro, L.A., Gonzalez, A., Chandel, N.S., Hersam, M.C., 2011. Minimizing oxidation and stable nanoscale dispersion improves the biocompatibility of graphene in the lung. Nano. Lett. 11 (12), 5201.
Ermakov, A., Popov, A., Ermakova, O., Ivanova, O., Baranchikov, A., Kamenskikh, K., Shekunova, T., Shcherbakov, A., Popova, N., Ivanov, V., 2019. The first inorganic mitogens: Cerium oxide and cerium fluoride nanoparticles stimulate planarian regeneration via neoblastic activation. Mater. Sci. Eng. C. 104, 109924.
Gao, L., Li, A., Lv, Y., Huang, M., Liu, X., Deng, H., Liu, D., Zhao, B., Liu, B., Pang, Q., 2021. Planarian gamma-interferon-inducible lysosomal thiol reductase (GILT) is required for gram-negative bacterial clearance. Dev. Comp. Immunol. 116, 103914.
Gao, T., Sun, B., Xu, Z., Chen, Q., Yang, M., Wan, Q., Song, L., Chen, G., Jing, C., Zeng, E. Y., Yang, G., 2022. Exposure to polystyrene microplastics reduces regeneration and growth in planarians. J. Hazard. Mater. 432, 128673.
Guo, Z., Zhang, P., Chetwynd, A.J., Xie, H.Q., Valsami-Jones, E., Zhao, B., Lynch, I., 2020. Elucidating the mechanism of the surface functionalization dependent neurotoxicity of graphene family nanomaterials. Nanoscale 12 (36), 18600–18605.
Hagstrom, D., Cochet-Escartin, O., Zhang, S., Khuu, C., Collins, E.M.S., 2015. Freshwater planarians as an alternative animal model for neurotoxicology. Toxicol. Sci. 147 (1), 270–285.
Hagstrom, D., Cochet-Escartin, O., Collins, E., 2016. Planarian brain regeneration as a model system for developmental neurotoxicology. Regeneration 3 (2), 65–77.
Hashemi, E., Akhavan, O., Shamsara, M., Daliri, M., Dashtizad, M., Farmany, A., 2016. Synthesis and cyto-genotoxicity evaluation of graphene on mice spermatogonial stem cells. Colloids Surf. B: Biointerfaces 146, 770–776.
Hoyle, C., Rivers-Auty, J., Lemarchand, E., Vranic, S., Wang, E., Buggio, M., Rothwell, N. J., Allan, S.M., Kostarelos, K., Brough, D., 2018. Small, Thin Graphene Oxide Is Anti-inflammatory Activating Nuclear Factor Erythroid 2-Related Factor 2 via Metabolic Reprogramming. ACS Nano 12 (12), 11949–11962.
Hu, X., Wei, Z., Mu, L., 2017. Graphene oxide nanosheets at trace concentrations elicit neurotoxicity in the offspring of zebrafish. Carbon 117, 182–191.
Inoue, T., Hoshino, H., Yamashita, T., Shimoyama, S., Agata, K., 2015. Planarian shows decision-making behavior in response to multiple stimuli by integrative brain function. Zool. Lett. 1 (1), 1–15.
Kapu, M.M., Schaeffer, D.J., 1991. Planarians in toxicology. Responses of asexualDugesia dorotocephala to selected metals. Bull. Environ. Contam. Toxicol. 47 (2), 302–307.
Kim, Y., Jeong, J., Yang, J., Joo, S.-W., Hong, J., Choi, J., 2018. Graphene oxide nano-bio interaction induces inhibition of spermatogenesis and disturbance of fatty acid metabolism in the nematode. Caenorhabditis elegans.Toxicology 410, 83–95.
Kluever, A.N., Aungst, J., Gu, Y., Hatwell, K., Shackelford, M., 2014. Infant toxicology: State of the science and considerations in evaluation of safety. Food Chem. Toxicol. 70 (2), 68–83.
Knakievicz, T., 2014. Planarians as invertebrate bioindicators in freshwater environmental quality: the biomarkers approach. Ecotoxicol. Environ. Contam. 9 (1), 1–12.
Kourie, J.I., 1998. Interaction of reactive oxygen species with ion transport mechanisms. Am. J. Physiol. Cell. Physiol. 275 (1), C1–C24.
Kumar, S., Raj, S., Sarkar, K., Chatterjee, K., 2016. Engineering a multi-biofunctional composite using poly(ethylenimine) decorated graphene oxide for bone tissue regeneration. Nanoscale 6820.
Leynen, N., Van Belleghem, F.G., Wouters, A., Bove, H., Ploem, J.-P., Thijssen, E., Langie, S.A., Carleer, R., Ameloot, M., Artois, T., 2019. In vivo toxicity assessment of silver nanoparticles in homeostatic versus regenerating planarians. Nanotoxicology 13 (4), 476–491.
Li, N., Zhang, X., Song, Q., Su, R., Zhang, Q., Kong, T., Liu, L., Jin, G., Tang, M., Cheng, G., 2011. The promotion of neurite sprouting and outgrowth of mouse hippocampal cells in culture by graphene substrates. Biomaterials 32 (35), 9374–9382.
Li, P., Xu, T., Wu, S., Lei, L., He, D., 2017. Chronic exposure to graphene-based nanomaterials induces behavioral deficits and neural damage in Caenorhabditis elegans. J. Appl. Toxicol. 37 (10), 1140–1150.
Li, Y., Liu, Y., Fu, Y., Wei, T., Le Guyader, L., Gao, G., Liu, R.-S., Chang, Y.-Z., Chen, C., 2012. The triggering of apoptosis in macrophages by pristine graphene through the MAPK and TGF-beta signaling pathways. Biomaterials 33 (2), 402–411.
Lim, S.Y., Davidson, S.M., Hausenloy, D.J., Yellon, D.M., 2007. Preconditioning and postconditioning: The essential role of the mitochondrial permeability transition pore. Cardiovasc. Res 42 (6). S171-S171.
Little, S., Johnston, H.J., Stone, V., Fernandes, T.F., 2021. Acute waterborne and chronic sediment toxicity of silver and titanium dioxide nanomaterials towards the oligochaete, Lumbriculus variegatus. NanoImpact 21, 100291.
Liu, Y., Luo, Y., Wu, J., Wang, Y., Yang, X., Yang, R., Wang, B., Yang, J., Zhang, N., 2013. Graphene oxide can induce in vitro and in vivo mutagenesis. Sci. Rep. 3 (1), 1–8.
López-Dolado, E., González-Mayorga, A., Portolés, M.T., Feito, M.J., Ferrer, M.L., Del Monte, F., Gutiérrez, M.C., Serrano, M.C., 2015. Subacute tissue response to 3D graphene oxide scaffolds implanted in the injured rat spinal cord. Adv. Healthc. Mater. 4 (12), 1861–1868.
Lovrić, J., Bazzi, H.S., Cuie, Y., Fortin, G.R., Winnik, F.M., Maysinger, D., 2005. Differences in subcellular distribution and toxicity of green and red emitting CdTe quantum dots. J. Mol. Med. (Berl., Ger.) 83 (5), 377–385.
Lu, X., Feng, X., Werber, J.R., Chu, C., Zucker, I., Kim, J.H., Osuji, C.O., Elimelech, M., 2017. Enhanced antibacterial activity through the controlled alignment of graphene oxide nanosheets. Proc. Natl. Acad. Sci. USA, 201710996.
Lv, M., Zhang, Y., Liang, L., Wei, M., Hu, W., Li, X., Huang, Q., 2012. Effect of graphene oxide on undifferentiated and retinoic acid-differentiated SH-SY5Y cells line. Nanoscale 4 (13), 3861–3866.
Ma, B., Guo, S., Nishina, Y., Bianco, A., 2021b. Reaction between graphene oxide and intracellular glutathione affects cell viability and proliferation. ACS Appl. Mater. Interfaces 13 (3), 3528–3535.
Ma, J., Liu, R., Wang, X., Liu, Q., Chen, Y., Valle, R.P., Zuo, Y.Y., Xia, T., Liu, S.J., 2015. Crucial role of lateral size for graphene oxide in activating macrophages and stimulating pro-inflammatory responses in cells and animals. ACS nano 9 (10), 10498–10515.
Ma, J.; Liu, X.; Yang, Y.; Qiu, J.; Dong, Z.; Ren, Q.; Zuo, Y.Y.; Xia, T.; Chen, W.; Liu, S.J. A. n, Binding of Benzo [a] pyrene alters the bioreactivity of fine biochar particles toward macrophages leading to deregulated macrophagic defense and autophagy. 2021a, 15, (6), 9717–9731.
Malina, T., Maršálková, E., Holá, K., Zbořil, R., Maršálek, B., 2020. The environmental fate of graphene oxide in aquatic environment—Complete mitigation of its acute toxicity to planktonic and benthic crustaceans by algae. J. Hazard. Mater. 399, 123027.
Mao, H.Y., Laurent, S., Chen, W., Akhavan, O., Imani, M., Ashkarran, A.A., Mahmoudi, M., 2013. Graphene: promises, facts, opportunities, and challenges in nanomedicine. Chem. Rev. 113 (5), 3407–3424.
Meng, L., Yang, X., Ren, J., Qu, K., Qu, X., 2012. Using graphene oxide high near-infrared absorbance for photothermal treatment of Alzheimer's disease. Adv. Mater. 24 (13), 1722–1728.
Murugadoss, S., van den Brule, S., Brassinne, F., Sebaihi, N., Mejia, J., Lucas, S., Petry, J., Godderis, L., Mast, J., Lison, D., 2020. Is aggregated synthetic amorphous silica toxicologically relevant? Part. Fibre Toxicol. 17 (1), 1–12.
Ofoegbu, P.U., Lourenço, J., Mendo, S., Soares, A.M., Pestana, J.L., 2019. Effects of low concentrations of psychiatric drugs (carbamazepine and fluoxetine) on the freshwater planarian, Schmidtea mediterranea. Chemosphere 217, 542–549.
Park, S.Y., Park, J., Sim, S.H., Sung, M.G., Kim, K.S., Hong, B.H., Hong, S., 2011. Enhanced differentiation of human neural stem cells into neurons on graphene. Adv. Mater. 23 (36), H263–H267.
Pellettieri, J., Fitzgerald, P., Watanabe, S., Mancuso, J., Green, D.R., Alvarado, A.S., 2010. Cell death and tissue remodeling in planarian regeneration. Dev. Biol. 338 (1), 76–85.
Perera, F., Herbstman, J., 2011. Prenatal environmental exposures, epigenetics, and disease. Reprod. Toxicol. 31 (3), 363–373.
Pieper, H., Chercheja, S., Eigler, S., Halbig, C.E., Filipovic, M.R., Mokhir, A., 2016. Endoperoxides revealed as origin of the toxicity of graphene oxide. Angew. Chem. Int. Ed. 55 (1), 405–407.
Pirotte, N., Stevens, A.-S., Fraguas, S., Plusquin, M., Van Roten, A., Van Belleghem, F., Paesen, R., Ameloot, M., Cebrià, F., Artois, T., 2015. Reactive oxygen species in planarian regeneration: an upstream necessity for correct patterning and brain formation. Oxid. Med. Cell. Longev. 2015.
Prá, D., Lau, A.H., Knakievicz, T., Carneiro, F.R., Erdtmann, B., 2005. Environmental genotoxicity assessment of an urban stream using freshwater planarians. Mutat. Res. /Genet. Toxicol. Environ. Mutagen. 585 (1–2), 79–85.
Pulido, C., Ryan, T.A., 2021. Synaptic vesicle pools are a major hidden resting metabolic burden of nerve terminals. Sci. Adv. 7 (49), eabi9027.
Qi, Y., Wei, S., Xin, T., Huang, C., Pu, Y., Ma, J., Zhang, C., Liu, Y., Lynch, I., Liu, S.J., 2022. Passage of exogeneous fine particles from the lung into the brain in humans and animals. Proc. Natl. Acad. Sci. U.S.A. 119 (26), e2117083119.
Raffa, R.B., Valdez, J.M., 2001. Cocaine withdrawal in Planaria. Eur. J. Pharmacol. 430 (1), 143–145.
Rivera, V., Perich, M., 1994. Effects of water quality on survival and reproduction of four species of planaria (Turbellaria: Tricladida). Invertebr. Reprod. Dev. 25 (1), 1–7.
Ross, K.G., Currie, K.W., Pearson, B.J., Zayas, R.M., 2017. Nervous system development and regeneration in freshwater planarians. Wiley Interdisciplinary Reviews: Developmental Biology 6 (3), e266.
Russell, W.M.S., Burch, R.L., 1959. The principles of humane experimental technique [M]. Methuen.
Salvetti, A., Rossi, L., Iacopetti, P., Li, X., Nitti, S., Pellegrino, T., Mattoli, V., Golberg, D., Ciofani, G., 2015. In vivo biocompatibility of boron nitride nanotubes: effects on

stem cell biology and tissue regeneration in planarians. Nanomedicine 10 (12), 1911–1922.
Sasidharan, A., Swaroop, S., Chandran, P., Nair, S., Koyakutty, M., 2016. Cellular and molecular mechanistic insight into the DNA-damaging potential of few-layer graphene in human primary endothelial cells. Nanomed.: Nanotechnol., Biol. Med. 12 (5), 1347–1355.
Seabra, A.B., Paula, A.J., de Lima, R., Alves, O.L., Durán, N., 2014. Nanotoxicity of graphene and graphene oxide. Chem. Res. Toxicol. 27 (2), 159–168.
Seifert, A.W., Muneoka, K., 2018. The blastema and epimorphic regeneration in mammals. Dev. Biol. 433 (2), 190–199.
Serrano, R., 1989. Structure and function of plasma membrane ATPase. Annu. Rev. Plant Biol. 40 (1), 61–94.
Shahnawaz Khan, M., Abdelhamid, H.N., Wu, H.F., 2015. Near infrared (NIR) laser mediated surface activation of graphene oxide nanoflakes for efficient antibacterial, antifungal and wound healing treatment. Colloids Surf. B Biointerfaces 127, 281–291.
Shang, L., Qi, Y., Lu, H., Pei, H., Zhang, W., 2019. Graphene and graphene oxide for tissue engineering and regeneration. Thera Bionanomater. 165–185.
Sharifi, S., Behzadi, S., Laurent, S., Forrest, M.L., Stroeve, P., Mahmoudi, M., 2012. Toxicity of nanomaterials. Chem. Soc. Rev. 41 (6), 2323–2343.
Shibata, N., Rouhana, L., Agata, K., 2010. Cellular and molecular dissection of pluripotent adult somatic stem cells in planarians. Dev. Growth Differ. 52 (1), 27–41.
Umesono, Y., Watanabe, K., Agata, K., 1999. Distinct structural domains in the planarian brain defined by the expression of evolutionarily conserved homeobox genes. Dev. Genes Evol. 209 (1), 31–39.
Wang, K., Ruan, J., Song, H., Zhang, J., Wo, Y., Guo, S., Cui, D., 2011. Biocompatibility of graphene oxide. Nanoscale Res Lett. 6 (1), 1–8.
Xiaoli, F., Yaqing, Z., Ruhui, L., Aijie, C., Yanli, Z., Lili, C., Longquan, S., 2021. Graphene oxide disrupted mitochondrial homeostasis through inducing intracellular redox deviation and autophagy-lysosomal network dysfunction in SH-SY5Y cells. J. Hazard. Mater., 126158
Xie, C., Zhang, P., Guo, Z., Li, X., Pang, Q., Zheng, K., He, X., Ma, Y., Zhang, Z., Lynch, I., 2020. Elucidating the origin of the surface functionalization-dependent bacterial toxicity of graphene nanomaterials: Oxidative damage, physical disruption, and cell autolysis. Sci. Total Environ. 747, 141546.
Xiong, S., Luo, J., Wang, Q., Li, Z., Li, J., Liu, Q., Gao, L., Fang, S., Li, Y., Pan, H., 2020. Targeted graphene oxide for drug delivery as a therapeutic nanoplatform against Parkinson's disease. Biomater. Sci. 9 (5), 1705–1715.
Yuan, Z., Zhang, J., Tu, C., Wang, Z., Xin, W., 2016. The protective effect of blueberry anthocyanins against perfluorooctanoic acid-induced disturbance in planarian (Dugesia japonica). Ecotoxicol. Environ. Saf. 127, 170–174.
Zhang, B., Yu, Q., Zhang, Y.-M., Liu, Y., 2019. Two-dimensional supramolecular assemblies based on β-cyclodextrin-grafted graphene oxide for mitochondrial dysfunction and photothermal therapy. Chem. Commun. 55 (81), 12200–12203.
Zhang, J., Yuan, Z., Zheng, M., Sun, Y., Wang, Y., Yang, S., 2013. Effects of N, N-dimethylformamide on behaviour and regeneration of planarian Dugesia japonica. Toxicol. Ind. Health. 29 (8), 753–760.
Zhang, P., He, X., Ma, Y., Lu, K., Zhao, Y., Zhang, Z., 2012. Distribution and bioavailability of ceria nanoparticles in an aquatic ecosystem model. Chemosphere 89 (5), 530–535.
Zhang, P., Selck, H., Tangaa, S.R., Pang, C., Zhao, B., 2017b. Bioaccumulation and effects of sediment-associated gold-and graphene oxide nanoparticles on Tubifex tubifex. J. Environ. Sci. 51, 138–145.
Zhang, P., Guo, Z., Luo, W., Monikh, F.A., Xie, C., Valsami-Jones, E., Lynch, I., Zhang, Z., 2020. Graphene oxide-induced pH alteration, iron overload, and subsequent oxidative damage in rice (Oryza sativa L.): A new mechanism of nanomaterial phytotoxicity. Environ. Sci. Technol. 54 (6), 3181–3190.
Zhang, X., Zhou, Q., Zou, W., Hu, X., 2017a. Molecular mechanisms of developmental toxicity induced by graphene oxide at predicted environmental concentrations. Environ. Sci. Technol. 51 (14), 7861–7871.
Zhang, Y., Ali, S.F., Dervishi, E., Xu, Y., Li, Z., Casciano, D., Biris, A.S., 2010. Cytotoxicity effects of graphene and single-wall carbon nanotubes in neural phaeochromocytoma-derived PC12 cells. ACS nano 4 (6), 3181–3186.